Phase I Trial of ^{131}I-GMIB-Anti-HER2-VHH1, a New Promising Candidate for HER2-Targeted Radionuclide Therapy in Breast Cancer Patients

Matthias D'Huyvetter[1,2], Jens De Vos[1], Vicky Caveliers[2,3], Ilse Vaneycken[3], Johannes Heemskerk[3], Francois P. Duhoux[4], Christel Fontaine[5], Marian Vanhoeij[6], Albert D. Windhorst[7], Frank van der Aa[7], N. Harry Hendrikse[7], Jos L.E. Eersels[1,2], Hendrik Everaert[3], Pieterjan Gykiere[3], Nick Devoogdt[1,2], Geert Raes[1,8,9], Tony Lahoutte[1–3], and Marleen Keyaerts[2,3]

[1]Precirix NV/SA, Brussels, Belgium; [2]In Vivo Cellular and Molecular Imaging Laboratory, Vrije Universiteit Brussel, Brussels, Belgium; [3]Nuclear Medicine Department, UZ Brussel, Brussels, Belgium; [4]Medical Oncology Department, King Albert II Cancer Institute, Cliniques Universitaires Saint-Luc and Institut de Recherche Expérimentale et Clinique, Université Catholique de Louvain, Brussels, Belgium; [5]Department of Medical Oncology, UZ Brussel, Brussels, Belgium; [6]Department of Oncological Surgery, UZ Brussel, Brussels, Belgium; [7]Department of Radiology and Nuclear Medicine, Amsterdam UMC, Vrije Universiteit Amsterdam, Amsterdam, The Netherlands; [8]Lab of Cellular and Molecular Immunology, Vrije Universiteit Brussel, Brussels, Belgium; and [9]Myeloid Cell Immunology Lab, VIB Center for Inflammation Research, Brussels, Belgium

^{131}I-GMIB-anti-human epidermal growth factor receptor type 2 (HER2)-VHH1 is a targeted radionuclide theranostic agent directed at HER2-expressing cancers. VHH1 is a single-domain antibody covalently linked to therapeutic ^{131}I via the linker *N*-succinimidyl 4-guanidino-methyl-3-iodobenzoate (SGMIB). The phase I study was aimed at evaluating the safety, biodistribution, radiation dosimetry, and tumor-imaging potential of ^{131}I-GMIB-anti-HER2-VHH1 in healthy volunteers and breast cancer patients. **Methods:** In a first cohort, 6 healthy volunteers were included. The biodistribution of ^{131}I-GMIB-anti-HER2-VHH1 was assessed using whole-body (anterior and posterior) planar images obtained at 40 min and at 2, 4, 24, and 72 h after intravenously administered (38 ± 9 MBq) ^{131}I-GMIB-anti-HER2-VHH1. Imaging data were analyzed using OLINDA/EXM software to determine the dosimetry. Blood and urine samples were obtained over 72 h. In the second cohort, 3 patients with metastatic HER2-positive breast cancer were included. Planar whole-body imaging was performed at 2 and 24 h after injection. Additional SPECT/CT images were obtained after the whole-body images at 2 and 24 h if there was relevant uptake in known cancer lesions. **Results:** No drug-related adverse events were observed throughout the study. The biologic half-life of ^{131}I-GMIB-anti-HER2-VHH1 in healthy subjects was about 8 h. After intravenous administration, the compound was eliminated from the blood with a 2.5-h half-life. The drug was eliminated primarily via the kidneys. The drug was stable in circulation, and there was no increased accumulation in the thyroid or stomach. The absorbed dose to the kidneys was 1.54 ± 0.25 mGy/MBq, and to bone marrow it was 0.03 ± 0.01 mGy/MBq. SPECT/CT imaging in patients with advanced breast cancer showed focal uptake of ^{131}I-GMIB-anti-HER2-VHH1 in metastatic lesions. **Conclusion:** Because of its favorable toxicity profile and its uptake in HER2-positive lesions, this radiopharmaceutical can offer new therapeutic options to patients who have progressed on trastuzumab, pertuzumab, or trastuzmab emtansine, given its difference in mode-of-action. A dose escalation is planned in a subsequent phase I/II study to assess the therapeutic window of this compound (NCT04467515).

Received Aug. 28, 2020; revision accepted Nov. 11, 2020.

For correspondence or reprints, contact Marleen Keyaerts (marleen.keyaerts@vub.be).

Published online December 4, 2020.

Key Words: single-domain antibody; 131I; breast cancer; theranostics

J Nucl Med 2021; 62:1097–1105
DOI: 10.2967/jnumed.120.255679

Single-domain antibodies (sdAbs) are the antigen-binding units derived from natural light-chain–deficient camelid antibodies. Compared with conventional antibodies and their antibody fragments, sdAbs are smaller (15 kDa) and can bind antigens on hidden or unusual epitopes. sdAbs are considered low-immunogenic, have nanomolar affinities, and can be produced in high yields (*1,2*).

Tumor cell membrane antigens represent an important target for anticancer treatment. Theoretically, sdAbs can be generated against virtually any cancer-specific membrane-associated protein, such as HER2 or CD20, and bear unusually beneficial properties for targeted radionuclide therapy (*3–8*). The human epidermal growth factor receptor type 2 (HER2) is a typical example of a membrane receptor that may be overexpressed on the cell membrane of breast, ovarian, and gastric carcinoma (*9*). Activation of this receptor stimulates cancer cell proliferation, resulting in increased cell mobility and less apoptosis. Consequently, HER2 overexpression is associated with tumor aggressiveness and an increased probability for recurrent disease. Targeted therapies for HER2 are clinically used, such as monoclonal antibodies (trastuzumab and pertuzumab) that specifically bind the extracellular domain of HER2, specific tyrosine kinase inhibitors (lapatinib) that interact with the intracellular domain of HER2, or antibody–drug conjugates derived from monoclonal antibodies. Information on the HER2 status of tumors is therefore of major importance since it has an enormous impact on the therapy selection. At present, HER2 expression is assessed using tissue biopsies. However, even with such patient selection, treatment failure still occurs, either immediately or via acquired resistance. New-generation anti-HER2 agents, such as antibody–drug conjugates, have shown therapeutic efficacy in patients in whom antibody-based or tyrosine kinase

inhibitor–based therapy regimens already failed, exemplifying the potential of improved HER2 treatment agents.

Anti-HER2-VHH1, also referred to as sdAb 2Rs15d, targets the HER2 receptor and was selected as a lead compound because of superior characteristics and the fact that it does not compete with binding of trastuzumab and pertuzumab (*10*). In its radionuclide therapy formulation, it introduces a novel mechanism of action to the landscape of HER2-targeted treatments.

^{68}Ga-labeled anti-HER2-VHH1 (^{68}Ga-NOTA-HER2) is under clinical development for the detection of HER2 expression in known tumoral sites using PET. A first-in-humans trial in 20 breast cancer patients using this tracer was successfully conducted (*11,12*), and multiple phase II trials are ongoing. No treatment-related adverse events were observed. The main conclusions were that ^{68}Ga-DOTA-HER2 PET/CT is a safe procedure, with radiation doses comparable to other PET/CT procedures, and that imaging reveals whole-body expression of HER2 in primary tumors and metastases.

Preclinical studies with ^{131}I-labeled anti-HER2-VHH1 (^{131}I-GMIB-anti-HER2-VHH1) were conducted evaluating the potential of this compound as a therapeutic agent for targeted radionuclide therapy. In these preclinical studies, the tumor-targeting characteristics and in vivo blood clearance of the compound were similar to those of the ^{68}Ga-labeled compound. Surprisingly, the biodistribution profile for ^{131}I-GMIB-anti-HER2-VHH1 was more favorable, with kidney uptake much lower than for ^{68}Ga-NOTA-HER2. The absorbed dose delivered to the tumor remained high and was higher than to the kidney. This favorable biodistribution, combined with the theranostic characteristics of ^{131}I, has now triggered interest in using this compound as a potential targeted radionuclide therapy agent in metastatic patients with HER2 positivity (*13*). ^{131}I-GMIB-anti-HER2-VHH1 at a low injected activity could be used for confirming accumulation in HER2-positive disease, followed by several cycles with ^{131}I-GMIB-anti-HER2-VHH1 at a high injected activity for therapy. Here, we present the first-in-human results with low-injected-activity ^{131}I-GMIB-anti-HER2-VHH1 to assess safety, tolerability, biodistribution, dosimetry, and tumor uptake in healthy volunteers and in HER2-positive breast cancer patients.

MATERIALS AND METHODS

Preparation of ^{131}I-GMIB-Anti-HER2-VHH1

All reagents and solvents were obtained from commercial suppliers and were of high-performance liquid chromatography (HPLC) grade or analytic grade and used as such. *N*-succinimidyl 4-[N^1,N^2-Bis(Boc)-guanidino-methyl]-3-trimethylstannyl)benzoate (precursor for iodination) and *N*-succinimidyl 4-guanidino-methyl-3-iodobenzoate (SGMIB) as a reference standard were obtained from ABX Chemicals in freeze-dried 50-μg aliquots. Radioiodide ($Na^{131}I$, no carrier added; specific activity of >55.5 GBq/μmol) in 0.05 M NaOH was obtained from GE Healthcare.

To obtain ^{131}I-SGMIB, 0.20 mL of 2% acetic acid in acetonitrile, 50 μg of SGMIB precursor dissolved in 0.10 mL of acetonitrile, and *N*-chlorosuccinimide (400 μg) in 50 μL of acetonitrile were added to 50 μL of Na[^{131}I]I-solution (1,924 ± 273 MBq) and reacted for 15 min at room temperature. After labeling, the reaction mixture was dried at 50°C under a gentle N_2 flow. For removal of the Boc-protecting groups, 0.15 mL of trifluoroacetic acid was added and allowed to react for 15 min. After deprotection, traces of trifluoroacetic acid were removed from the deprotected reaction mixture by adding 0.10 mL of acetonitrile, followed by evaporation. To the dried ^{131}I-SGMIB, 2.0 mL of eluent were added and injected onto an HPLC column for semipreparative HPLC purification of ^{131}I-SGMIB. Semipreparative HPLC purification consisted of the following components and parameters: 2.0 mL/min; a 19/81 acetonitrile/4 mM NaH_2PO_4 mobile phase; a Symmetry RP-18 (Waters) 300 × 7.8 mm, 7-μm column; and a 254-nm ultraviolet wavelength. The collected ^{131}I-SGMIB was further concentrated by means of a solid-phase extraction cartridge (tC18 Plus [Waters], preconditioned with 5 mL of acetonitrile and 10 mL of water) and eluted in 1.0 mL of 1% acetic acid/acetonitrile. ^{131}I-SGMIB was obtained in a radiochemical yield of 32.2% ± 7.4%.

Purified ^{131}I-SGMIB was dried, and 0.10 mg of anti-HER2-VHH1 in 0.10 mL of 0.1 M borate buffer (pH 8.5) was added for conjugation during 25 min. The conjugated reaction mixture was diluted with 0.7 mL of formulation buffer (ascorbic acid, 5 mg/mL, in 0.9% NaCl, pH 5.2) and loaded onto a PD-10 column for purification. Another 2.0 mL of formulation buffer were added and discarded. ^{131}I-GMIB-anti-HER2-VHH1 was collected by eluting with 3.0 mL of formulation buffer.

A panel of analytic tests was performed, including visual inspection, pH, radiochemical purity, binding affinity, sterility filter membrane integrity, bacterial endotoxins, and sterility. All analytic procedures are validated and adequate to detect significant deviations from the specifications. In short, visual inspection was performed after final sterile filtration to confirm that the solution was clear and colorless. The pH of the drug product was determined by pH electrode. Radiochemical purity was determined using instant thin-layer chromatography and size-exclusion chromatography, equipped with ultraviolet and radioactivity detection. As the eluent for instant thin-layer chromatography, 20 mM citric acid with 10% of acetonitrile was used. In parallel, analysis via size-exclusion chromatography consisted of the following components and parameters: 0.75 mL/min; 50 mM sodium phosphate; 0.15 M NaCl; 10 mM NaN_3, pH 6.6; GE Healthcare Superdex Peptide 10/300 GL column; run time of 60 min; and 280-nm ultraviolet wavelength. Endotoxin levels were assessed by use of a Food and Drug Administration–licensed *Limulus* amebocyte lysate test system according to the instructions provided by the supplier (Endosafe-PTS; Charles River). The filter integrity test was performed using the bubble-point method, according to the European Pharmacopoeia. The integrity of the sterile end-filter was tested as part of the manufacturing process. Sterility testing was performed according to the European Pharmacopoeia on a nonradioactive-medium fill. Antigen binding was assessed through the Lindmo assay using HER2-positive SKOV-3 cells. The incubation was done overnight at room temperature on a shaking device.

Study Design and Approvals

This was a single-center, open-label, nonrandomized first-in-humans clinical trial. The trial design is depicted in Figure 1. The study was approved by the Belgian Federal Agency for Medicines and Health Products, the regional ethics committee of Universitair Ziekenhuis Brussel, and the radiation protection agency of Belgium and was registered with the identifiers EudraCT 2015-004840-21 and NCT02683083. The study was conducted in accordance with the Declaration of Helsinki and the International Conference on Harmonization Guidelines for Good Clinical Practice. Written informed consent was obtained from all participants.

The study was performed in 2 parts, with part 1 including 6 healthy volunteers. After approval by the independent Data Safety Monitoring Board, 3 breast cancer patients were included in part 2 to assess uptake of ^{131}I-GMIB-anti-HER2-VHH1 in metastatic lesions.

Study Population, Inclusion, and Thyroid Blockage

Six healthy Caucasian volunteers (5 women, 1 man) were included to assess safety, biodistribution, and dosimetry, and 3 breast cancer

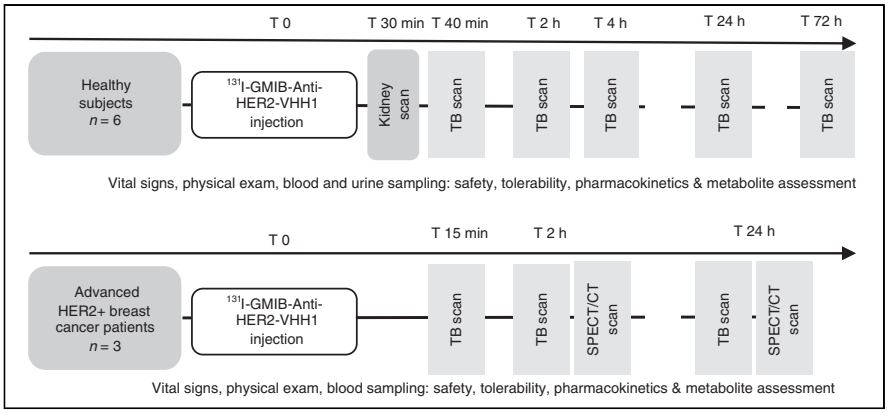

FIGURE 1. Clinical trial design. T = time; TB = total body.

patients (2 women, 1 man, aged ≥18 y) were included to assess uptake in metastatic lesions.

Patients with local, locally advanced, or metastatic HER2-positive breast carcinoma (defined as either an immunohistochemistry score of 3+ or in situ hybridization–amplified) were included.

Key exclusion criteria for both subgroups were pregnancy or lactation, any contraindication to thyroid blockage with potassium iodine, abnormal liver function (alanine aminotransferase/aspartate aminotransferase > 2 times the upper limit of normal; bilirubin > 1.5 times the upper limit of normal) or kidney function (estimated glomerular filtration rate < 50 mL/min/1.73 m^2), serious active infection, a recent gastrointestinal disorder with diarrhea, other life-threatening illness, inability to communicate reliably or give informed consent, potential difficulty cooperating with the requirements of the study, or previous participation in this study or a previous study with anti-HER2 VHH1. In addition, healthy volunteers were excluded if they had clinically significant disease or previous thyroid disorders. For part 2, patients with at least 1 lesion minimally 15 mm in diameter were studied to assess uptake of ^{131}I-GMIB-anti-HER2-VHH1 in metastatic lesions.

Study Medications

For thyroid blockage, 130 mg of potassium iodide daily were administered orally for 4 consecutive days starting 24 h before the administration of ^{131}I-GMIB-anti-HER2-VHH1. The dose range in the study protocol was a single-dose continuous infusion of 50 ± 40 μg with a radioactivity range of 46 ± 28 MBq for healthy subjects and 64 ± 46 MBq for patients. The radiopharmaceutical was administered over 5 min via a peripheral intravenous line using an infusion pump. The empty syringe and intravenous line were measured for residual radioactivity after injection. The subjects did not void until after completion of the first whole-body planar scan. All subjects fasted for at least 4 h before receiving the dose.

Safety Assessment

Vital parameters (blood pressure, heart rate, and temperature) were monitored throughout the study. Hematologic and metabolic panels (hemoglobin, white blood cells, neutrophils, lymphocytes, platelets, creatinine, blood urea nitrogen, calcium, sodium, potassium, carbon dioxide, lactate dehydrogenase, alanine transaminase, aspartate aminotransferase, alkaline phosphatase, total bilirubin, and albumin) were obtained before and at 24 h after injection of ^{131}I-GMIB-anti-HER2-VHH1. Subjective adverse events were assessed using open questions before injection, throughout the time that subjects were present in the nuclear medicine department, and at subsequent visits up to 24 h after injection for patients and up to 72 h after injection for healthy volunteers.

Planar and SPECT/CT Imaging

Images were acquired using a Philips BrightView XCT equipped with high-energy general-purpose collimators; the photopeak was set at 364 keV (20% window, scatter windows of 6%). Whole-body images were acquired at 10 cm/min. The matrix size was 512 by 1,024 pixels, and the pixel size was 2.8 mm. Whole-body images were acquired at 40 min and at 2, 4, 24, and 72 h for healthy volunteers and at 15 min and at 2 and 24 h for patients.

During whole-body image acquisitions, a source of known activity of ^{131}I was positioned between the lower legs of the subject. The distance between the camera bed and each camera head was kept constant for each subject. In healthy volunteers, dynamic acquisitions over the liver and kidneys took place during the injection and up to 30 min after the start of the injection.

SPECT/CT was optional after whole-body imaging at 2 and 24 h in patients, as decided by the primary investigator on the basis of uptake in known cancer lesions. SPECT/CT acquisitions consisted of 64 projections of 40 s, in step-and-shoot mode, with a matrix of 128 by 128 pixels and a pixel size of 4.7 mm. Scatter was corrected by scaled subtraction of the scatter-window projection images before reconstruction, and reconstruction was performed using the manufacturer's proprietary iterative reconstruction algorithm (Astonish) (*14*). Reconstructed images had 4.7-mm isotropic voxels. CT images were acquired (120 kV, 80 mA) for localization and attenuation correction.

Blood and Urine Samples

Pharmacokinetics in the blood were assessed using radioactive counting of blood and plasma samples over time. In healthy volunteers, blood samples were taken from a peripheral vein before injection; at 5, 10, 30, 60, 105, and 225 min after injection; and at 24 and 72 h after injection. Urine sample were collected at about 60 and 225 min and at 24 and 72 h after injection. Whole-blood and plasma samples were counted against appropriate standards of known dilution in an automatic γ-well counter and, after correction for decay and background activity, expressed as percentage injected activity. The blood volume of each volunteer was estimated according to body weight and height, using the Nadler formula and the patient's hematocrit. Blood half-lives were calculated with a 2-phase exponential decay model using Prism (GraphPad Software).

Plasma at preselected time points and urine aliquots from 5 healthy volunteers and 3 patients were analyzed by size-exclusion chromatography or reversed-phase HPLC to identify possible metabolites. The HPLC system consisted of a Hitachi Chromaster (VWR) equipped with a pump with a low-pressure gradient system, a 6-channel degasser, a manual injector, a Flowstar LB513 radioactive detector (Berthold), and a Hitachi Chromaster ultraviolet detector. Data were acquired using the Flowstar software.

Each sample was injected on a Superdex 75 5/150 GL column (GE Healthcare) at room temperature. The mobile phase consisted of 50 mM sodium phosphate, 0.15 M NaCl, and 0.01 M NaN_3. Analysis was performed at a flow rate of 0.3 mL/min with an isocratic program using a 20-min run time.

Region-of-Interest Definition and Dosimetry

The uptake of ^{131}I-GMIB-anti-HER2-VHH1 in different organs was determined from anterior and posterior whole-body images (by calculating the geometric mean). Regions of interest were drawn (whole body, brain, lungs, liver, kidneys, thyroid, heart, intestines,

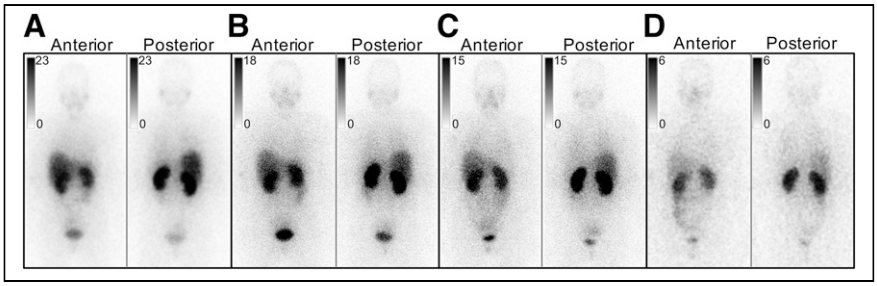

FIGURE 2. Biodistribution of ^{131}I-GMIB-anti-HER2-VHH1 in healthy volunteer 3 after 40 min (A), 2 h (B), 4 h (C), and 24 h (D). Anterior and posterior images from skull to thighs are displayed per time point. Images at 72 h showed only faint kidney and bladder activity and were therefore omitted. Images were individually scaled (inverted gray scale expressed in counts per pixel) to allow maximal visualization of distribution at each time point. Uptake intensity is moderate throughout time points in kidneys and liver and low in salivary glands. Increasing level of large-bowel activity might indicate low level of intestinal clearance.

bladder, and thigh muscle) using Osirix software (Pixmeo SARL). For dosimetry calculations, OLINDA/EXM software, version 1.0 (*14*), was used. A biexponential fit was used; excretion parameters were set at 95% for renal excretion and 4.8 h for the voiding bladder interval. Both male and female adult models were applied on every healthy subject, regardless of the sex of the subject. Averages of all 6 healthy volunteers are reported per sex.

RESULTS

Preparation of ^{131}I-GMIB-Anti-HER2-VHH1

The radiopharmaceutical was produced at Amsterdam UMC according to current good-manufacturing-practice guidelines. ^{131}I-GMIB-anti-HER2-VHH1 (n = 9) was obtained in a yield of 6.1% ± 1.7% calculated from Na^{131}I with an average total synthesis time of 3 h 44 ± 28 min. One batch contained 83 ± 20 MBq of ^{131}I-GMIB-anti-HER2-VHH1 in a sterile, isotonic, and pyrogen-free solution for intravenous injection. The pH of the final drug-product solution ranged from 5.2 to 5.6. ^{131}I-GMIB-anti-HER2-VHH1 was obtained at a ^{131}I-SGMIB–to–sdAb molar ratio of (0.09 ± 0.02) to 1.0. Radiochemical purity after synthesis (n = 9) was measured to be 97.8% ± 3.2% via instant thin-layer chromatography and 99.7% ± 0.5% via size-exclusion chromatography, whereas the Lindmo assay revealed an immunoreactive fraction of 73.9% ± 9.5%. After 24 h, radiochemical purity was calculated to be 96.4% ± 2.5% by instant thin-layer chromatography and 97.4% ± 1.4% by size-exclusion chromatography. The mean administered activity of ^{131}I-GMIB-anti-HER2-VHH1 was 38.1 ± 8.8 MBq (range, 24.7–49.7 MBq) for healthy volunteers and 60.7 ± 4.3 MBq (range, 56.9–65.3 MBq) for patients, with a protein amount ranging from 10 to 90 μg of anti-HER2 VHH1 for all participants.

Subject Characteristics, Safety, and Tolerability

All subjects were fully compliant with the oral intake of potassium iodide for thyroid blockade. Subject demographics are provided in Supplemental Table 1. In healthy volunteers, 4 adverse events of mild intensity were recorded (ecchymosis, adhesive plaster sensitivity, or abdominal discomfort). In patients, no adverse events were noted. All adverse events were considered unrelated or likely unrelated to the study drug. There were no adverse drug reactions or clinically detectable pharmacologic effects in any of the 9 subjects. No significant changes in vital signs or laboratory parameters were observed.

Dynamic, Whole-Body Imaging in Healthy Subjects

Given the fast pharmacokinetics of sdAbs, dynamic imaging of the upper abdomen was performed (30 images of 1 min each) to evaluate the initial kidney activity. Representative images and relative mean time–activity curves are shown in Supplemental Figure 1. Although absolute kidney uptake varied between subjects, the dynamics were very reproducible over all 6 investigated subjects. An initial fast uptake was seen over the first 10 min, followed by a slow increase.

Representative whole-body images of a healthy volunteer from 40 min to 24 h after injection are shown in Figure 2. Geometric mean images of all other subjects are shown in Supplemental Figure 2. The most intense uptake was visible in the kidneys and, in a variable degree, in the liver. Faint uptake was observed in the salivary glands and intestines. In all subjects, faint activity in the region of the colon could be seen at 24 h after injection (Supplemental Fig. 3), indicating a minor level of gastrointestinal uptake or excretion. No uptake was visible in the thyroid or stomach (as expected because of blockade by potassium iodide), brain, muscle, or normal breast tissue. Uptake in organs was measured using 5 whole-body imaging time points, and average uptake values are shown in Supplemental Table 2.

Whole-body clearance over 72 h was calculated on the basis of the activity remaining in the body of healthy volunteers, excluding any bladder activity, over time. Using a monoexponential curve fit, the biologic half-life was calculated from these data for each healthy subject and averaged 7.72 ± 1.40 h (Fig. 3).

Blood and Urine Sample Analysis in Healthy Subjects

On average, 97.48% ± 1.85% of ^{131}I-GMIB-anti-HER2-VHH1 was in the plasma fraction at 60 min after injection. The blood clearance in healthy volunteers is shown in Figure 4. A

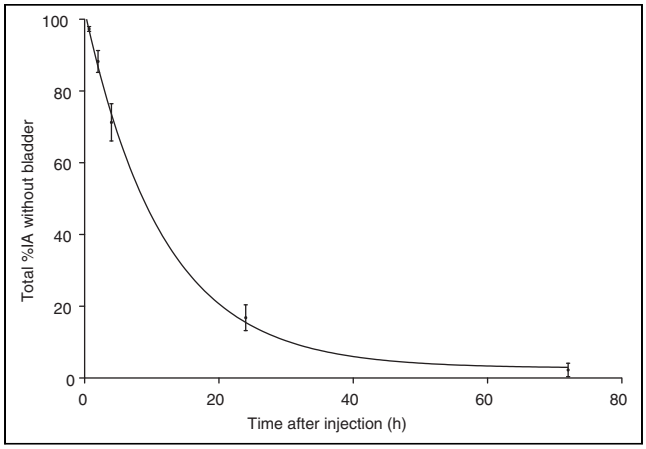

FIGURE 3. Total-body clearance of ^{131}I-GMIB-anti-HER2-VHH1 in healthy subjects. Data shown are without urinary activity present in bladder. IA = injected activity.

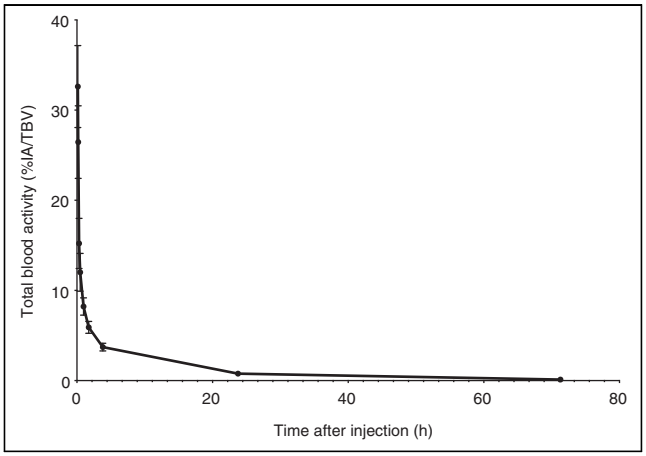

FIGURE 4. Blood clearance of ^{131}I-GMIB-anti-HER2-VHH1 in healthy subjects. Data shown represent mean ± SD for total blood activities of 6 subjects. IA = injected activity; TBV = total blood volume.

biexponential curve fit resulted in a distribution phase to the tissues with a mean half-life of 6.70 ± 1.13 min and an elimination phase from the body with a half-life of 150.80 ± 35.69 min. For 1 subject, the sample obtained at 10 min was omitted for this analysis because it revealed a higher value than the sample at 5 min, and this was considered a procedural error.

Metabolites were analyzed in the blood of healthy subjects at 5 different time points. On a total of 30 samples, there was only 1 sample that showed a measurable metabolite peak on HPLC analysis. It was a blood sample at 1 h after injection, with no detectable metabolites in the subsequent blood samples at 4, 24, and 72 h after injection. To further substantiate the absence of metabolites in the blood, additional metabolite analysis was performed in the subsequent 3 patients. No metabolites were detected in these patients' samples 1 h after injection. In urine samples, up to 3 different metabolites were detected in all subjects until 24 h after injection and in 1 subject until 72 h. Further identification of metabolites was not part of this study.

TABLE 1
Mean Organ Doses and Mean Effective Dose of 6 Healthy Subjects

	Mean absorbed dose (mGy/MBq)	
Target organ	Male	Female
Adrenals	0.057 ± 0.016	0.074 ± 0.020
Brain	0.008 ± 0.003	0.010 ± 0.003
Breasts	0.022 ± 0.012	0.029 ± 0.016
Gallbladder wall	0.051 ± 0.015	0.061 ± 0.019
LLI wall	0.479 ± 0.061	0.521 ± 0.067
Small intestine	0.046 ± 0.017	0.057 ± 0.020
Stomach wall	0.037 ± 0.016	0.046 ± 0.020
ULI wall	0.041 ± 0.016	0.053 ± 0.021
Heart wall	0.051 ± 0.014	0.062 ± 0.018
Kidneys	1.50 ± 0.25	1.63 ± 0.27
Liver	0.127 ± 0.038	0.168 ± 0.050
Lungs	0.074 ± 0.009	0.095 ± 0.012
Muscle	0.031 ± 0.014	0.039 ± 0.018
Ovaries		0.069 ± 0.021
Pancreas	0.049 ± 0.016	0.061 ± 0.021
Red marrow	0.032 ± 0.013	0.038 ± 0.015
Osteogenic cells	0.052 ± 0.029	0.069 ± 0.038
Skin	0.022 ± 0.012	0.028 ± 0.015
Spleen	0.050 ± 0.016	0.062 ± 0.021
Testes	0.032 ± 0.014	
Thymus	0.026 ± 0.014	0.033 ± 0.018
Thyroid	0.160 ± 0.048	0.193 ± 0.059
Urinary bladder wall	0.764 ± 0.012	1.04 ± 0.01
Uterus		0.074 ± 0.021
Total body	0.042 ± 0.014	0.053 ± 0.018
Effective dose (mSv/MBq)	0.174 ± 0.019	0.212 ± 0.022

LLI = lower large intestines; ULI = upper large intestines.
Values are expressed as mean ± SD (n = 6).

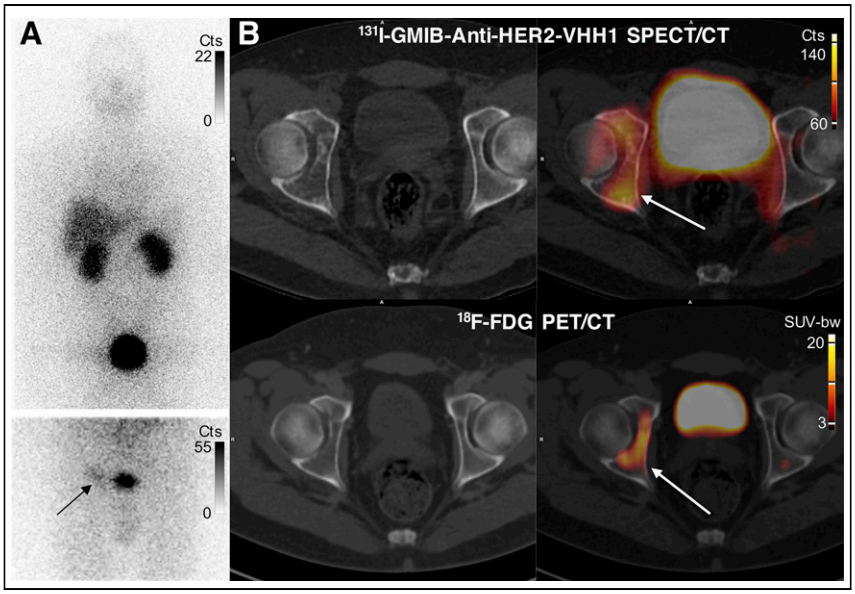

FIGURE 5. Images of uptake in bone metastasis in patient 1. (A) Anterior planar whole-body images 2 h after injection. Image at top shows pronounced bladder activity, and image below (static anterior image over pelvis after bladder voiding) shows moderate tracer uptake (arrow) lateral to urinary bladder. (B) SPECT/CT and PET/CT images at 2.5 h after ^{131}I-GMIB-anti-HER2-VHH1 injection and 1 h after ^{18}F-FDG injection, respectively, showing increased uptake in right acetabular bone (arrows) as well as bladder activity (urinary excretion). ^{18}F-FDG PET/CT images were obtained 44 d before ^{131}I-GMIB-anti-HER2-VHH1 injection. Cts = counts; SUV-bw = standardized uptake value - body weight.

Region-of-Interest Definition and Dosimetry in Healthy Subjects

Dosimetry values for individual organs, as well as whole-body estimated absorbed dose, are shown in Table 1 as the average for 6 healthy volunteers. The organs showing the highest absorbed doses were the kidneys, followed by the urinary bladder wall and the lower large intestine. The absorbed dose to the kidneys was 1.63 mGy/MBq in women. The bone marrow absorbed dose of 0.038 mGy/MBq in women was low.

Tumor Uptake in Cancer Patients

Patient 1 was a 43-y-old man with a recent diagnosis of metastatic (bone) estrogen receptor–positive and HER2-positive breast cancer. The patient had started first-line treatment with trastuzumab–pertuzumab–docetaxel and had received the second cycle 8 d before a ^{131}I-GMIB-anti-HER2-VHH1 injection. Focal uptake was seen at the site of a 33-mm (largest axis) bone metastasis in the right acetabulum (Fig. 5). Treatment was continued, resulting in a partial metabolic response on ^{18}F-FDG PET/CT imaging after the fourth cycle.

Patient 2 was a 77-y-old woman with a recent history of ER-positive HER2-positive breast cancer and a metastasis in the sternal bone. Her first evaluation under treatment with trastuzumab–pertuzumab–paclitaxel showed progressive disease with extension of the sternal lesion to the clavicular bone and the first left rib, as well as new liver metastases (all liver metastases $<$ 15 mm in size). Two days after the last monoclonal antibody treatment, she participated in this clinical trial. After injection of ^{131}I-GMIB-anti-HER2-VHH1, the planar whole-body scan and SPECT/CT showed focal uptake in the large sternal metastasis, persisting until 24 h after injection (Fig. 6). Uptake in this sternal lesion was calculated using region-of-interest analysis on planar imaging as 1.6% injected activity at 2 h.

Patient 3 was a 61-y-old woman with ER-positive HER2-positive breast cancer. She was receiving first-line treatment with paclitaxel–trastuzumab–pertuzumab for distant lymph node invasion in the mediastinum and retroperitoneum and pleural disease at the time of inclusion. Planar whole-body imaging with ^{131}I-GMIB-VHH1, administered 21 d after trastuzumab–pertuzumab injection, did not show lesional uptake. On SPECT/CT, only faint tracer accumulation was visible in the subcarinal lymph node and in a pleural metastasis (Fig. 7).

DISCUSSION

Targeted radionuclide therapy is an attractive therapeutic modality wherein a labeled moiety selectively targets cancer cells and may deliver a lethal payload from a decaying radionuclide. However, intact antibodies might not be ideal vectors because of their large size (~150 kDa), resulting in suboptimal pharmacokinetics, poor tumor penetration, and slow normal-tissue clearance (*15*). Efforts to optimize the pharmacokinetics of larger vectors, such as pretargeting, are gaining more attention. Because of their high specificity of binding, subnanomolar affinity, and low immunogenicity, sdAbs are attractive probes for imaging and radionuclide therapy. Their small size (10–15 kDa), compared with intact antibodies, facilitates tumor penetration and rapid elimination from blood and normal tissues (*16*). SdAbs have been directed to a variety of transmembrane cancer cell molecular targets to image or treat cancer in preclinical or clinical models of breast (*12,13*) and ovarian cancer (*5*), multiple myeloma (*4*), and non-Hodgkin lymphoma (*6*).

The rationale for clinical translation of ^{131}I-GMIB-anti-HER2-VHH1 is 5-fold. First, the use of ^{131}I-SGMIB as a prosthetic group results in a stable drug product in vivo, with no associated dehalogenation as compared with direct radioiodination methods based on IODO-GEN (Thermo Fisher Scientific) (*17*). Second, preclinical studies have indicated that ^{131}I-GMIB-anti-HER2-VHH1 at a high injected activity has a therapeutic effect and that accumulation in kidneys remains significantly lower than for radiometal-based analogs (*5,13*). Third, HER2-targeting VHH1 targets a unique epitope and does not compete with trastuzumab and pertuzumab, thus allowing the use of ^{131}I-GMIB-VHH1 in patients who undergo HER2-targeted therapies (*10,13*). Fourth, ^{131}I-GMIB-anti-HER2-VHH1 brings a novel mechanism of action to the field of HER2-targeted therapeutics. Fifth, the theranostic character with low-injected-activity radioiodine or PET labels such as ^{68}Ga/^{18}F allows selection of patients, based on imaging, who are likely to benefit from high-injected-activity radioiodine treatments (*18*).

This first-in-human application of the radioiodinated sdAb ^{131}I-GMIB-anti-HER2-VHH1 demonstrated no drug-related adverse events in healthy volunteers or patients at low injected activities. The radiopharmaceutical was well tolerated by all study subjects. There were no clinically relevant changes in vital signs, physical examination findings, or blood parameters. The biologic half-life

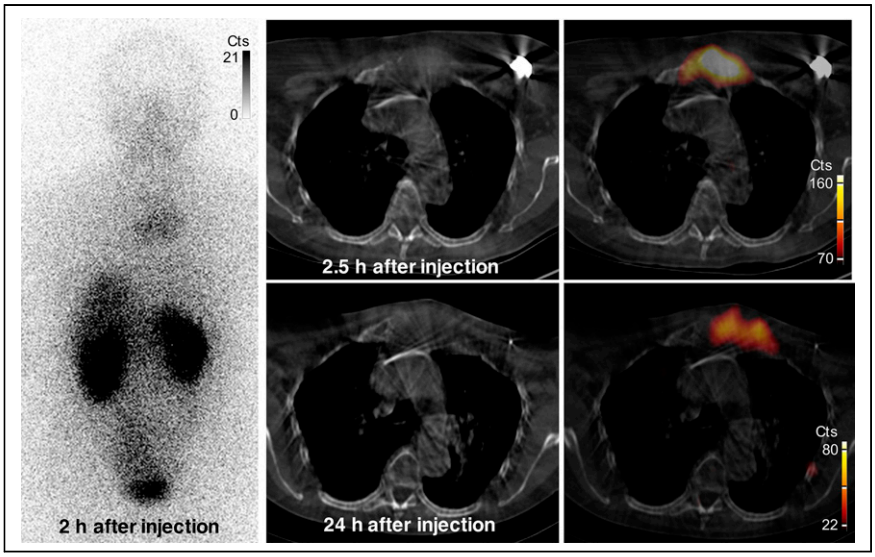

FIGURE 6. Images of uptake in bone metastasis in patient 2. Anterior whole-body (left) and SPECT/CT (right) images show uptake of ^{131}I-GMIB-anti-HER2-VHH1 at level of large lytic bone metastasis, with soft-tissue component at sternal bone both at 2.5 h and at 24 h after injection. Small differences in area of uptake are explained by differences in patient positioning (arms up at 2.5 h and arms down at 24 h, to maximize patient comfort). Cts = counts.

of ^{131}I-GMIB-anti-HER2-VHH1 was about 8 h. More than 95% of the drug was present in the plasma fraction of blood, with a fast plasma elimination half-life of 2.5 h, and no general trends of metabolization in blood were seen. The consistent presence of metabolites in urine indicates renal metabolization. The product specifications obtained before intravenous injection confirmed that no significant free iodine was injected.

^{131}I-GMIB-anti-HER2-VHH1 showed a favorable biodistribution and was eliminated primarily via the kidneys and only to a minor extent via the intestinal tract. At 40 min after intravenous injection, on average 24% of ^{131}I-GMIB-anti-HER2-VHH1 was in the kidneys and 14% was in the liver. The washout from these organs was fast, with only 4% in the kidney and 2% in the liver at 24 h. The thyroid and stomach showed no specific accumulation, as was expected because the patients were pretreated with potassium iodide for blockage.

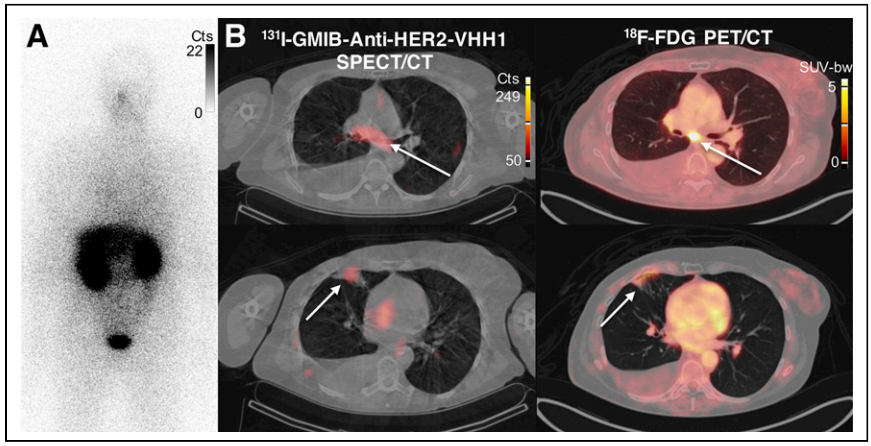

FIGURE 7. Images of patient 3 showing metabolically active sites of disease at subcarinal lymph node and pleural metastasis. (A) Anterior whole-body planar image at 2 h after injection showing no focal uptake in thoracic region. (B) Uptake (arrows) of ^{131}I-GMIB-anti-HER2-VHH1 at 2.5 h after injection is weak and close to background activity in 13-mm subcarinal lymph node (top) and pleural metastasis (bottom). Cts = counts; SUV-bw = standardized uptake value - body weight.

^{131}I-GMIB-anti-HER2-VHH1 proved to be safe after a single injection, with the protein amount ranging from 10 to 90 mg and an average injected activity of 60.7 MBq (range, 24.7–65.3 MBq). Dosimetry analysis predicts that the dose-limiting organ will be the kidneys, receiving the highest absorbed dose of 1.62 mGy/MBq. As described by Santoro et al. (*19*), no clear cumulative absorbed dose cutoff has been identified in peptide receptor radionuclide therapy with ^{177}Lu to predict the risk of organ failure. Reports often refer to 23 Gy for the kidneys and 2 Gy for the bone marrow, although these values were obtained with fractionated external-beam radiation therapy (*19*). The administration of 15 GBq would lead to an absorbed dose of 23 Gy to the kidneys. Bone marrow is the most radiosensitive tissue in the body. ^{131}I-GMIB-anti-HER2-VHH1 results in a low-level bone marrow exposure (0.038 mGy/MBq). This level of irradiation would occur only after administration of 59.0 GBq of ^{131}I-GMIB-anti-HER2-VHH1. Therefore, kidney toxicity and hematotoxicity are unlikely to occur in the planned dose escalation study of ^{131}I-GMIB-anti-HER2-VHH1 (1.85–7.4 GBq). ^{131}I-GMIB-anti-HER2-VHH1 at an injected activity of 7.4 GBq would deliver to the kidneys and bone marrow absorbed doses well below the defined levels of 23 Gy for kidney and 2 Gy for bone marrow typically accepted by regulatory agencies for therapeutic radiopharmaceuticals. The current study was performed without kidney protection measures such as arginine/lysine infusion before and after drug administration, a method routinely used in peptide receptor radionuclide therapy (e.g., ^{177}Lu-DOTATATE [Lutathera; Novartis]). Preclinical studies with radiolabeled sdAbs show that the administration of succinylated gelatine (Gelofusine; B. Braun) or positively charged amino acids can reduce kidney retention levels by more than 40% (*5,20*). Consequently, introduction of this amino acid infusion before and after drug administration could potentially double the maximal tolerable dose.

As a secondary objective in this phase I study, tumor uptake was evaluated in 3 patients with HER2-positive breast cancer. Uptake was clearly present in 2 patients with lesions larger than 3 cm; in a third patient with smaller lesions, low-level uptake could be visualized, likely because of partial-volume effects. The strongest uptake was seen in a patient with progressive disease at the time of study drug administration. In patient 1, a known bone metastasis larger than 3 cm in the right acetabulum was visualized on planar and SPECT/CT images at both early time points after injection as well as after 24 h. In patient 2, focal uptake was observed in a known sternal bone metastasis larger than 3 cm through total-body scans and through SPECT/CT images taken at 2 and 24 h.

The focal drug accumulation in the cancer lesion contrasted sharply with surrounding tissues. Patient 3 had no lesions larger than 3 cm, and only low-level uptake was identified by visual interpretation of the scan. The therapeutic value of this compound will be assessed in the planned phase I/II dose escalation and expansion study (NCT04467515). Centralized production through an optimized process will allow for a steady supply of ^{131}I-GMIB-anti-HER2-VHH1 to multiple clinical sites that take part in this study.

We previously described the preclinical evaluation of ^{131}I-GMIB-anti-HER2-VHH1 (*13*). That study showed ^{131}I-GMIB-anti-HER2-VHH1 to be cleared quickly in mice via the kidneys, with only minor activity in the liver. The data presented in the current study indicate that the biodistribution and pharmacokinetic data in humans are very similar to the data predicted from preclinical experiments. Optimal biodistribution in combination with proven preclinical efficacy in models of breast and ovarian cancer form the basis for further clinical investigation of ^{131}I-GMIB-anti-HER2-VHH1. Moreover, a preclinical model of HER2-positive brain metastases showed better survival after treatment with ^{131}I-GMIB-anti-HER2-VHH1 than after trastuzumab. Indeed, these results indicate that the small size of sdAbs allows more efficient targeting beyond the breached blood–brain barrier compared with full-size antibodies such as trastuzumab (*21*).

CONCLUSION

The human data on a radioiodinated sdAb for therapeutic intent support the translational potential of radiolabeled sdAbs in general and ^{131}I-GMIB-anti-HER2-VHH1 in particular, beyond imaging purposes. Dosimetry predicts the kidneys to be the dose-limiting organ on dose escalation, but kidney toxicity should occur at only very high injected activities. The uptake in HER2-positive lesions further supports therapeutic potential and opens new therapeutic options for patients who progress on trastuzumab, pertuzumab, or trastuzumab emtansine, given the distinct mode of action of ^{131}I-GMIB-anti-HER2-VHH1. The results of this study prompted a multicenter dose escalation and therapeutic clinical investigation (NCT04467515) of ^{131}I-GMIB-anti-HER2-VHH1 in patients with HER2-positive breast and gastric cancer.

DISCLOSURE

Marleen Keyaerts and Tony Lahoutte are senior clinical investigators and Matthias D'Huyvetter is postdoctoral researcher of the Research Foundation-Flanders. Francois Duhoux received a postdoctoral clinical mandate (2017-034) from the Foundation Against Cancer. This research was funded by Innoviris.Brussels (RBC/2014-R-75). Geert Raes, Nick Devoogdt, and Tony Lahoutte are consultants for Precirix NV/SA and, together with Matthias D'Huyvetter and Jens De Vos, hold ownership interest in Precirix NV/SA. Marleen Keyaerts, Geert Raes, Nick Devoogdt, and Tony Lahoutte hold ownership interest in Abscint NV/SA. Tony Lahoutte is a member of the scientific advisory board of Ion Beam Applications (IBA) and a member of the strategic committee of the Institute of RadioElements (IRE). Marleen Keyaerts has received travel and accommodation expenses from Bayer NV. Nick Devoogdt has received funding for preclinical research from Boehringer-Ingelheim, Complix, Confo Therapeutics, Roche, 121BIO, Agenus, and Telix Pharma. Marleen Keyaerts, Nick Devoogdt, Marleen D'Huyvetter, Jens De Vos, Tony Lahoutte, and Geert Raes have patents on sdAb imaging and therapy. Francois Duhoux holds advisory/consultancy roles for Amgen, AstraZeneca, Daiichi Sankyo, Eli Lilly, Novartis, Pfizer, Pierre Fabre, Roche, and Teva (paid to the institution, outside the submitted work); has received speaker fees from Eli Lilly, Mundi Pharma, Novartis, Pfizer, and Roche (paid to the institution, outside the submitted work); and has received travel support from Amgen, Pfizer, Roche, and Teva. No other potential conflict of interest relevant to this article was reported.

ACKNOWLEDGMENTS

We thank the study coordinator, Yasmine De Maeyer, and the nurses and technologists, Gratienne Van Holsbeeck, Wendy Kemps, Nadine Eersels, Kathleen Op Debeeck, Carl Van Halewijn, Annick Luppens, Claudia Housen, and Viviane Janssens, for their valuable help in this trial. We also thank Peter Covens and Frank De Geeter as members of the Data Safety Monitoring Board.

KEY POINTS

QUESTION: Is ^{131}I-GMIB-anti-HER2-VHH1 a candidate for HER2-targeted radionuclide therapy in breast cancer patients?

PERTINENT FINDINGS: ^{131}I-GMIB-anti-HER2-VHH1 was found to be safe, to be stable after administration, and to clear rapidly from the blood in healthy volunteers. The tracer accumulated in metastatic sites of patients with stage IV HER2-positive breast cancer.

IMPLICATIONS FOR PATIENT CARE: Because of its favorable toxicity profile and its uptake in HER2-positive lesions, this radiopharmaceutical can offer new therapeutic options to patients who have progressed on trastuzumab, pertuzumab, or trastuzumab emtansine, given its different mode of action.

REFERENCES

1. Krasniqi A, D'Huyvetter M, Devoogdt N, et al. Same-day imaging using small proteins: clinical experience and translational prospects in oncology. *J Nucl Med.* 2018;59:885–891.
2. Lecocq Q, De Vlaeminck Y, Hanssens H, et al. Theranostics in immuno-oncology using nanobody derivatives. *Theranostics.* 2019;9:7772–7791.
3. D'Huyvetter M, Aerts A, Xavier C, et al. Development of ^{177}Lu-nanobodies for radioimmunotherapy of HER2-positive breast cancer: evaluation of different bifunctional chelators. *Contrast Media Mol Imaging.* 2012;7:254–264.
4. Lemaire M, D'Huyvetter M, Lahoutte T, et al. Imaging and radioimmunotherapy of multiple myeloma with antiidiotypic nanobodies. *Leukemia.* 2014;28:444–447.
5. D'Huyvetter M, Vincke C, Xavier C, et al. Targeted radionuclide therapy with a ^{177}Lu-labeled anti-HER2 nanobody. *Theranostics.* 2014;4:708–720.
6. Krasniqi A, D'Huyvetter M, Xavier C, et al. Theranostic radiolabeled anti-CD20 sdAb for targeted radionuclide therapy of non-Hodgkin Lymphoma. *Mol Cancer Ther.* 2017;16:2828–2839.
7. Bolli E, D'Huyvetter M, Murgaski A, et al. Stromal-targeting radioimmunotherapy mitigates the progression of therapy-resistant tumors. *J Control Release.* 2019;314:1–11.
8. Puttemans J, Dekempeneer Y, Eersels JL, et al. Preclinical targeted α- and β^--radionuclide therapy in HER2-positive brain metastasis using camelid single-domain antibodies. *Cancers (Basel).* 2020;12:1017.
9. Vaneycken I, Devoogdt N, Van Gassen N, et al. Preclinical screening of anti-HER2 nanobodies for molecular imaging of breast cancer. *FASEB J.* 2011;25:2433–2446.
10. Lin NU, Winer EP. Brain metastases: the HER2 paradigm. *Clin Cancer Res.* 2007;13:1648–1655.
11. Xavier C, Vaneycken I, D'huyvetter M, et al. Synthesis, preclinical validation, dosimetry, and toxicity of ^{68}Ga-NOTA-anti-HER2 Nanobodies for iPET imaging of HER2 receptor expression in cancer. *J Nucl Med.* 2013;54:776–784.

12. Keyaerts M, Xavier C, Heemskerk J, et al. Phase I study of ^{68}Ga-HER2-Nanobody for PET/CT assessment of HER2 expression in breast carcinoma. *J Nucl Med.* 2016;57:27–33.
13. D'Huyvetter M, De Vos J, Xavier C, et al. ^{131}I-labeled anti- HER2 Camelid sdAb as a theranostic tool in cancer treatment. *Clin Cancer Res.* 2017;23: 6616–6628.
14. Seret A, Nguyen D, Bernard C. Quantitative capabilities of four state-of-the-art SPECT-CT cameras. *EJNMMI Res.* 2012;2:45.
15. D'Huyvetter M, Xavier C, Caveliers V, et al. Radiolabeled nanobodies as theranostic tools in targeted radionuclide therapy of cancer. *Expert Opin Drug Deliv.* 2014;18:1939–1954.
16. Debie P, Lafont C, Defrise M, et al. Size and affinity kinetics of nanobodies influence targeting and penetration of solid tumours. *J Control Release.* 2020;317:34–42.
17. Pruszynski M, Koumarianou E, Vaidyanathan G, et al. Improved tumor targeting of anti-HER2 nanobody through N-succinimidyl 4-guanidinomethyl-3-iodobenzoate radiolabeling. *J Nucl Med.* 2014;55:650–656.
18. Xavier C, Blykers A, Vaneycken I, et al. ^{18}F-nanobody for PET imaging of HER2 overexpressing tumors. *Nucl Med Biol.* 2016;43:247–252.
19. Santoro L, Mora-Ramirez E, Trauchessec D, et al. Implementation of patient dosimetry in the clinical practice after targeted radiotherapy using ^{177}Lu-[DOTA0, Tyr3]-octreotate. *EJNMMI Res.* 2018;8:103.
20. Gainkam LO, Caveliers V, Devoogdt N, et al. Localization, mechanism and reduction of renal retention of technetium-99m labeled epidermal growth factor receptor-specific nanobody in mice. *Contrast Media Mol Imaging.* 2011;6:85–92.
21. Marquez BV, Ikotun OF, Zheleznyak A, et al. Evaluation of ^{89}Zr-pertuzumab in breast cancer xenografts. *Mol Pharm.* 2014;11:3988–3995.